Published in final edited form as:
Ther Deliv. 2014 April ; 5(4): 467–486. doi:10.4155/tde.14.10.

Mechanisms of microbubble-facilitated sonoporation for drug and gene delivery

Zhenzhen Fan[‡,1], **Ronald E Kumon**[‡,2], and **Cheri X Deng**[*,3]

[1]Institute of Acoustics, Chinese Academy of Sciences, No. 21 Beisihuanxi Road, Beijing, 100190, China

[2]Department of Physics, Kettering University, 1700 University Avenue, Flint, MI, 48504-6214, USA

[3]Department of Biomedical Engineering, University of Michigan, 2200 Bonisteel Boulevard, Ann Arbor, MI, 48109, USA

Ultrasound-mediated delivery facilitated by microbubbles provides a novel means for intracellular drug and gene delivery and particularly a noninvasive strategy uniquely suitable for clinical applications. Spatiotemporally controllable application of ultrasound energy combined with microbubbles make it possible for site-specific delivery of therapeutic agents to the region-of-interest with minimal undesirable systemic side effects. By inducing rapid expansion/contraction and/or collapse of microbubbles, ultrasound application can temporarily increase the cell membrane permeability (sonoporation) to create a physical route for impermeable agents to enter the cells. Sonoporation is transient and dynamic, involving complex processes of bubble physics, bubble–cell interactions, and subsequent cellular effects that all affect the ultimate delivery outcome. This review summarizes the studies on the important aspects of the mechanisms of ultrasound-mediated delivery, provides illustrative examples of applications, and discusses the challenges and limitations of the technique. **Microbubbles** have been used for several decades as a contrast agent for **ultrasound** imaging [1]. The small size of microbubbles allows them access to well-perfused organs when injected into the vasculature, and their gas core efficiently reflects and scatters the incident ultrasound field, thereby increasing image contrast between the vasculature and the surrounding tissue. Recent developments in microbubble technology have enabled molecular imaging via targeting of the microbubbles to molecular markers of disease expressed on the surface of cells [2]. In addition to imaging, innovation in microbubbles has opened new opportunities for targeted drug and gene delivery. Ultrasound excitation of microbubbles has been exploited to increase vascular and cell membrane permeability and facilitate the passage of therapeutic agents across the vascular barrier and

[*]Author for correspondence: Tel.: +1 734 936 2855 Fax: +1 734 936 1905 cxdeng@umich.edu.
[‡]Authors contributed equally

Financial & competing interests disclosure
CX Deng acknowledges funding from the NIH (CA116592). The authors have no other relevant affiliations or financial involvement with any organization or entity with a financial interest in or financial conflict with the subject matter or materials discussed in the manuscript. This includes employment, consultancies, honoraria, stock ownership or options, expert testimony, grants or patents received or pending, or royalties. No writing assistance was utilized in the production of this manuscript.

cell membrane into the cytoplasm for drug and gene transfection [3–7]. The ultrasound delivery technique, with the advantage of noninvasive, spatiotemporaly controllable ultrasound application combined with functionalized micro-bubbles, holds great promise to provide new therapeutic strategies.

However, even with recent progress in the field, challenges remain, including relatively low delivery efficiency and large variation of delivery outcome. Better understanding of the underlying mechanisms is thus of great importance to optimize this technique and promote its translation towards clinical application.

Although the mechanisms of ultrasound- and microbubble-facilitated intracellular delivery have not yet been fully understood, a direct physical route of transport often termed **sonoporation** is most likely involved [8–10]. The dynamic response of the microbubbles driven by ultrasound as well as the interaction between the microbubbles and the cell membrane are key factors in determining delivery efficiency. Other factors such as the cellular response, the kinetics and metabolism of therapeutic agents in the cytoplasm, also play important roles in the ultimate outcome of ultrasound-mediated delivery. In this review, we first summarize progress in these aspects and then discuss limitations and challenges that the technique currently faces.

Responses of microbubbles to Ultrasound excitation

Due to the high compressibility of the gas core compared with the surrounding liquid medium, micro-bubbles are highly responsive to ultrasound excitation and exhibit robust dynamic behaviors under the influence of ultrasound [11]. The typical microbubbles used as ultrasound imaging contrast agents are engineered microbubbles with a water-insoluble gas core that is usually encapsulated with a thin layer made of lipid, polymer, or protein, with a thickness in the range of 10–100 nm [12]. Fluorinated gases are often used in the core because of their high permeation resistance into the surrounding fluid as compared with gases with lower molecular weights [13]. The encapsulating layer for commercially available microbubbles is typically composed of protein (e.g., denatured human albumin in Optison™) or lipid (e.g., Definity™, Sonovue™, Micromarker™), although polymer-based formulations have also been developed [14]. The encapsulating layer stabilizes the microbubbles and prolongs their lifetime by limiting gas diffusion and reducing the surface tension [15], therefore providing a reasonable time window for ultrasound imaging and therapy. Although the encapsulation layer alters the characteristics of microbubbles such as viscous damping and microbubble resonance frequency [16], encapsulated bubbles are still highly responsive to ultrasound excitations, exhibiting generally similar behaviors as free bubbles.

The most recent generation of microbubbles has been designed to target specific receptors on the cell surface [2]. These targeted microbubbles are typically constructed by attaching ligands to the encapsulating shell [17]. For example, in a lipid-based shell, small hydrophilic ligands can be attached to the distal end of the lipopolymer molecule via covalent bonding. Alternatively, a biotinylated ligand can be attached to a biotinylated microbubble via an avidin bridge. Ligands can include antibodies, peptides, and vitamins, depending on the

desired target and other immunogenic considerations [13]. In addition to targeting cells, ligands can also be used to attach desired payloads such as nanoparticles loaded with drugs or genes [18].

The dynamic activities of ultrasound excitation of microbubbles are critical in sonoporation. Without ultrasound stimulation, stationary microbubbles themselves alone do not generate any delivery, an observation that has been demonstrated by control experiments in numerous reported studies. Below we summarize the typical microbubble responses to ultrasound excitation.

Cavitation

During the alternating cycles of rarefaction and compression generated by an ultrasound field, microbubbles repeatedly expand and contract due to the change in acoustic pressure. The system is analogous to a driven mass on a spring, where the spring is the gas volume of the bubble, the mass is the inertia of the fluid surrounding the bubble, and the alternating acoustic pressure drives the system to oscillate. With low magnitudes of acoustic pressure, microbubbles exhibit stable **cavitation**, oscillating with relatively small amplitude around their equilibrium volume at the frequency of the ultrasound exposure, as modeled by the Rayleigh–Plesset equation and its related formulations [11]. If the microbubble is attached to a cell, then the expansion and contraction of the microbubble will push and pull on the cell, potentially leading to membrane opening (Figure 1A & B).

The rapid expansion and contraction of a microbubble can also generate fluid flow near the microbubble in the form of **microstreaming**. For example, in experiments performed with cells *in vitro*, the microbubbles are adjacent to the cell and a solid surface. Under these conditions, the acoustic pressure field induces a superposition of bubble volumetric oscillations and oscillatory translational motion of a bubble's center-of-mass [20]. This motion, together with the no-slip boundary condition at the solid surface, results in vortical bulk fluid flow (Figure 1D) [20,21]. This microstreaming results in shear stresses being exerted on the adjacent cells that can be sufficient in some cases to cause sonoporation [22,23].

When acoustic pressure is above a certain threshold, transient cavitation of microbubbles occurs with significant volume expansion (typically to more than twice of their original radius) and followed by collapse during compression. This transient cavitation is also called inertial cavitation, as the volumetric changes of the microbubbles no longer follow the frequency of incoming ultrasound but are dominated by the inertia of the surrounding liquid [11]. During the collapse, extremely high temperature and pressure can be generated in the center of the microbubble core, often accompanied by the generation of shock waves, high speed fluid microjets, reactive free radicals, and sometimes even photons (sonoluminescence) [8,24–27]. The existence of inertial cavitation in a volume can be detected acoustically by the elevated broadband noise level that occurs during bubble collapse [28–30]. Inertial cavitation has also been shown to be involved in the release of micelle-encapsulated drugs [31].

When a bubble is located near a solid surface, as when microbubbles are introduced near cells *in vitro*, induction of inertial cavitation by an acoustic wave can result in jetting [32–34]. During collapse of the bubble, the presence of the solid surface causes the fluid at the far side of the bubble from the solid surface to move differently from the fluid near the solid surface. This asymmetric movement of fluid can cause a jet of fluid to move through the center of the bubble toward the solid surface, resulting in a toroidal bubble, which eventually collapses or fragments due to its inherent instability [35]. For macroscopic (mm sized) bubbles, the high-speed of the jet can result in pitting or erosion of solid surfaces [36]. For microbubbles adjacent to cells, microjetting has been proposed as another mechanism for sonoporation (Figure 1C).

The use of ultrafast cameras with frame rates up to millions of frames/s has enabled direct optical observation of microbubble dynamics, greatly enhancing the understanding of the transient process of interaction between activated microbubble and cells. For example, imaging at 500 kframes/s showed that 4.5 μm-diameter microbubble next to a flat surface oscillated and imploded violently when exposed to ultrasound, forming a fluidic microjet directed toward the cell membrane of a cell cultured *in vitro* (Figure 2A) [8]. Still, others have argued that microjetting is not the dominant source of most sonoporation events based on computational and experimental analysis relating jet length to pore size [37,38]. Other studies showed that ultrasound could cause asymmetric oscillations, fragmentation, and jetting of microbubbles; bending and displacement of cells; and delivery of the extracellular agent propidium iodide (PI) [39,40]. PI is a 668.4 Da marker molecule often used for sonoporation studies because its fluorescence spectrum is shifted and significantly enhanced when it enters the cell and binds with intracellular nucleic acids. In another study, ultrafast photographs revealed that microbubbles underwent stable cavitation with the alternating expansion and contraction repeatedly disturbing the cell membrane, subsequently resulting in the intracellular uptake of PI (Figure 2B) [41]. A similar study with targeted microbubbles showed that sonoporation was induced when the relative vibration amplitude of the microbubbles was larger than 0.5 and with lower acoustic pressures than nontargeted microbubbles [42]. Moreover, direct optical evidence has demonstrated that microstreaming generated by a stably oscillating bubbles can entrain approaching lipid vesicles and later tear them up due to the high shear stresses induced [20]. Studies using commercially available nontargeted microbubbles (Optison™, Definity™) with passive acoustical cavitation detection have suggested that microstreaming is a more plausible explanation for sonoporation given that a significant level of sonoporation is observed when the peak rarefactional pressure is below the threshold for inertial cavitation [43–45]. However, it is important to keep in mind that measurements are often dependent on specific experimental configurations and spatial relationship of microbubbles with regard to cells. Differences in these aspects could lead to different values of ultrasound pressures responsible for sonoporation and cavitation.

While sonoporation studies have shown that the most significant results occur in the presence of microbubbles to initiate cavitation, it has also been hypothesized that ultrasound may induce intramembrane cavitation (‘bilayer sonophore’) under some conditions without

microbubbles, based on evidence from transmission electron microscopy (TEM) imaging [46].

Microbubble behaviors affected by acoustic radiation forces

In addition to cavitation, **acoustic radiation forces** associated with the incident ultrasound field also affect microbubbles and play a role in sonoporation. For example, we have demonstrated that single laser-generated bubbles can be directed toward a *Xenopus laevis* oocyte by use of the primary acoustic radiation force to push the bubble toward the cell prior to induction of cavitation, thereby allowing for study of the range of cavitation impact on cells [47]. More recently, a study has shown that microbubbles can be pushed into cells using primary acoustic radiation force at a low mechanical index, without causing inertial cavitation (Figure 1E) [19]. In addition, studies have shown that targeted microbubbles can be pushed by acoustic radiation force towards the vessel wall during ultrasound molecular imaging procedure, thus promoting binding of the targeted microbubbles and their retention at the diseased area [48,49]. To efficiently cause micro-bubble translation without causing bubble destruction, cavitation (volume expansion/contraction) of the microbubbles needs to be minimized by lowering the acoustic pressure and/or using driving frequencies away from the bubbles' resonance frequency along with longer exposure time.

If two or more microbubbles exist in the ultrasound field, then these microbubbles are also affected by secondary acoustic radiation forces, which result from the ultrasound scattered from other microbubbles within the incident ultrasound field. Driven by the secondary radiation force, microbubbles attract or repel from each other, depending on the phase of the volumetric oscillation. The secondary acoustic radiation force has been used to quantitatively investigate the binding force between receptors on a cell surface and the ligands on the targeted microbubble surface [50]. When multiple microbubbles are present in the vicinity of each other, secondary acoustic radiation force may cause them to move toward each other and form aggregates; when the acoustic pressure is high enough, microbubbles can fuse and form a large bubble [51]. Secondary acoustic radiation force can also cause adjacent targeted microbubbles bound to a functionalized substrate to attract and deform in a prolate shape with forces on the order of 1–2 nN, which is enough in some cases to pull out the lipid binding anchors from the microbubble shell [52]. These changes of microbubbles result in changes of their response and effects on cells, thereby significantly affecting ultrasound mediated delivery.

Ultrasound parameters & experimental setup affecting bubble activities & sonoporation

Investigation of single bubble dynamic behaviors in the microsecond time scale using ultrafast videomicroscopy has greatly increased our understanding of the transient cavitation process and its effect on sonoporation. However, the response of isolated microbubbles under highly controlled experimental conditions may differ significantly from the conditions that exist in realistic scenarios of practical applications, where the larger number of microbubbles, different ultrasound parameters (e.g., longer exposure times, diverse pulse repetition frequencies), and various geometries may all affect the bubble activities. Understanding of microbubble responses in such circumstances will be important to develop strategies to optimize the delivery outcome.

Microbubbles can exist and oscillate for thousands of cycles when driven by ultrasound pulses at low pressures (e.g., up to 20,000 cycles at 0.1 MPa), but they can also rapidly disappear when higher pressures are applied (e.g., lasting only up to 100 μs or 100 cycles at 0.4 MPa) [53]. In our recent study, we used a high speed camera (20 kframe/s) to continuously record microbubble dynamic activities driven by 1 s of pulsed ultrasound to examine the responses of a population of microbubbles to ultrasound application [54]. We observed diverse dynamics of microbubbles subjected to a wide range of ultrasound parameters. However, systematic analysis based on the rate of change of the bubble radius and the total bubble movement allowed us to identify three characteristic types of bubble dynamic behaviors including stable cavitation, translation and aggregation, and inertial cavitation (Figure 3). Inertial cavitation, which occurred when ultrasound pulses are short with high acoustic pressures (e.g., 8 μs pulse duration, 0.4 MPa acoustic pressure, 20 Hz pulse repetition frequencies, and 1 s total exposure), led to the highest rate of delivery and lowest cell death.

In addition to ultrasound parameters, geometrical configuration is another factor that can strongly influence microbubble response. Experiments *in vitro* have been conducted in centrifuge tubes or petri dishes, enclosed thin chambers (such as Opticell™), and cellulose tubes or vessels. In a centrifuge tube or petri dish, microbubbles were typically freely floating in the bulk solution. The random locations of micro-bubbles relative to cells may require long durations of ultrasound application (e.g., 0.1 to several seconds) to allow the direct interaction of microbubbles with cells to occur [55–57]. In experiments where a thin chamber was used, the cells were attached on the upper surface facing down, allowing the microbubbles to float up to be in close vicinity of cells. In this scenario, short ultrasound pulses (μs–ms time scale) may be sufficient to induce intracellular uptake [10,40–41]. For experiments where microbubbles were inside a microvessel with inner diameter comparable to the microbubble diameter, even a single short ultrasound pulse excitation (2 μs) was enough for the microbubble to exert influences on the vessel wall [58].

Transient delivery processes across the cell membrane

It has been repeatedly illustrated that one of the main routes for ultrasound-mediated intracellular delivery is the formation of reversible and nonspecific pores on cell membrane. The transient disruption of the cell membrane generates a physical pathway for impermeable extracellular agents to enter the cell cytoplasm.

Pore size

Direct physical evidence of membrane perforation has been obtained using scanning electron microscopy (SEM), which revealed the presence of pores with diameters from 100 nm to several micrometers [40,56,59–61,56]. Atomic force microscopy (AFM), TEM, and confocal fluorescence microscopy have confirmed plasma membrane discontinuities on ultrasound-treated cell surfaces, although the diameter of the disruption varies over a wide range, from several nanometers to scores of micrometers [8,9,60–62]. Representative images of pore formation captured using various techniques are shown in Figure 4. Higher acoustic pressures and longer exposure times have also been shown to generally create larger pores as measured by SEM and AFM [63,64]. Significant changes in surface topography changes

have been observed via AFM with peak-to-peak variation and surface roughness increasing after ultrasound treatment in the presence of microbubbles [62].

Care must be taken when interpreting results from imaging using these methods. As cells are typically fixed and prepared for imaging long after ultrasound exposure, pores may have already resealed completely or partially at the time of examination. Thus the images may not reveal the full or actual distribution of the pores generated during sonoporation for intracellular delivery.

Efforts have been made to estimate the pore size assuming that the pore is circular with a single ‘effective’ diameter and that passive diffusion is the predominant mechanism for transport into cell. Based on experimentally measured uptake of different-sized molecules at different times after ultrasound exposure, a model was constructed that predicted 150–300 μm pores closing with half-lives of 20–50 s [65]. Applying a quasi-steady electro-diffusion model to the measured transmembrane currents of single cells under a voltage clamp [66], our laboratory has estimated that the effective pore diameter was 110 ± 40 nm in *Xenopus laevis* oocytes using free microbubbles and ultrasound pulses of 0.1 s [66] and 15.7 ± 2.6 nm in HEK-293 cells using targeted microbubbles with ultrasound pulses of 8 μs [67]. We have also determined effective pore size by fitting a 2D diffusion model to the evolution of 2D fluorescence intensity of PI in cytoplasm over time (Figure 5B–E) [67]. Using this method, the maximum pore diameter was estimated to be from several nanometers to 100 nm.

Ultrasound conditions determine bubble behaviors, which in turn, determine the size of pores generated during sonoporation. In addition, different cell types may respond differently to the same ultrasound conditions both in terms of the poration and resealing processes, although there has been limited systematic study in this regard. In the studies using a postultrasound assay (such as SEM, TEM, AFM), the time point when the sonicated cell was fixed becomes another element that may induce variation in the pore size observed. Evidence also exists that ultrasound may be able to induce endocytosis, such that the intracellular uptake may not be due to physical pore formation entirely, particularly for transport of larger molecules (see the section “Nuclear membrane transport and gene expression for additional discussion”).

The dynamic process of pore formation & resealing

Due to the transient and microscopic nature of sonoporation, it is challenging to obtain real time information of pore formation and resealing. We have employed voltage-clamp and patch-clamp techniques as an novel strategy for real-time monitoring of sonoporation by measuring the transmembrane currents generated in single cells under voltage clamp [67–70]. When ultrasound was applied to generate sonoporation, the inward transmembrane current of a cell under voltage clamp increased as a result, indicating pore formation on the cell membrane. The recovery of the transmembrane current to its previous level indicates the resealing of the pore (Figure 5).

Our earlier studies using *Xenopus laevis* oocytes as a model system revealed two resealing processes (fast/early and slow/late processes) with different time constants, 0.11–0.21 s^{-1} for slow resealing and 0.79–1.19 s^{-1} for fast resealing [70]. Our recent study of HEK293

cells using targeted microbubbles confirmed that the dual exponential mathematical model can describe the resealing process, with the time constants for slow and fast process as 0.17 ± 0.05 s^{-1} and 4.21 ± 0.26 s^{-1}, respectively (Figure 5G & H) [67]. The similarity of slow time constants and difference in fast time constants may indicate cell-independent and cell-dependent mechanisms involved in pore resealing. The detailed origin of the two time scales is not entirely clear, but may reflect multiple different biophysical mechanisms acting during the resealing process, as discussed in the section “Mechanisms of cell membrane resealing” below.

Real-time spatiotemporal fluorescence measurements have also been used to directly relate pore formation with intracellular transport of an exogenous agent (e.g., PI). Typically intracellular fluorescence increases after ultrasound exposure, then decreases over 2–3 min, suggesting an initial permeation followed by efflux or metabolism of the PI [41]. In some experiments, intracellular fluorescence initially increases after ultrasound exposure but reaches a plateau, suggesting pore resealing without efflux of PI [10,41,67]. Unfortunately, the frame rate for fluorescence imaging is usually insufficient to resolve the multiple time scales observed in the electrophysiological recording. However, total PI fluorescence intensity has been shown to be correlated with the net electric charge across the membrane, supporting the hypothesis of diffusion-driven PI transport (Figure 5I) [67].

Mechanisms of cell membrane resealing

Different mechanisms may be involved for pore resealing depending on pore size generated in sonoporation. It has been proposed that exocytic events can facilitate the self-sealing potential inherent in a locally disordered lipid membrane as a result of wounding [71,72]. However, when large parts of the membrane must be replaced, a more complicated ‘patching’ processes, such as lysosome-mediated exocytosis or repair via specialized proteins and organelles, may be necessary. For example, after ultrasound treatment immunostaining has clearly shown that the lysosome specific protein, LAMP-1, was extended within the interior of insonated cells, and the cells closer to ultrasound-treated zone exhibited stronger LAMP-1 staining [73]. Another study showed similar results wherein disruption of the cell membrane evoked local exocytotic response utilizing lysosomes, as indicated by LAMP-1 staining [64].

Calcium ions (Ca^{2+}) have also been shown to play an important role in cell repair. The resealing process appears to require a minimum threshold of extracellular Ca^{2+}. The resealing process took longer at lower extra-cellular [Ca^{2+}] concentration, and cells failed to reseal when the extracellular Ca^{2+} was depleted [9,40,70,74]. Moreover, as shown by voltage-clamped current measurements of *Xenopus laevis* oocytes, the amplitude of the slow recovery process was unaffected by the extracellular [Ca^{2+}], whereas the amplitude of the fast process increased with increasing extracellular [Ca^{2+}], suggesting that the fast process is regulated by Ca^{2+}-dependent factor [70]. The corresponding rate constants for both the slow and fast processes were relatively unaffected by the extracellular [Ca^{2+}].

Nonspecific, size-dependent, bi-directional transport

Many studies have shown that sonoporation results in transport across the cell membrane that is nonspecific and driven by the concentration gradient. A wide range of agents have been observed to transport across the cell membrane, from ions to macromolecules, although with different characteristics depending on the size of the agents [9,65,75–76]. Molecules with smaller molecular weight (e.g., calcein, 623 Da; PI, 668 Da; fluorescein isothiocyanate (FITC)-dextran, 4400 Da) and physical size (e.g., calcein, 0.6 nm) were homogeneously distributed throughout the cytoplasm as well as in the nuclei after entering the cells, achieving concentrations comparable to the extracellular level. In contrast, molecules with larger molecular weight (150–2000 kDa, e.g., FITC-BSA, FITC-dextrans) and larger physical size (e.g., dextran-464, 18.5 nm) generally achieved lower concentrations compared with the extracellular concentration. The distribution inside the cells was less homogeneous with limited access to the nuclei. Reduced uptake of these agents with larger molecular weight is likely due to their lower diffusivity.

Bi-directional transport is another feature of sonoporation. Experiments have shown that the intracellular delivery of extracellular calcein is proportional to its extracellular concentration [9] and that cells preloaded with calcein and FITC-dextran will have reduced fluorescence levels of these dyes after sonication due to efflux of these molecules [9,76]. Loss of a preloaded calcium dye (fura-2) after single-pulse ultrasound exposure has also been observed [40]. We have reported real-time measurements showing that cells preloaded with fura-2 exhibited simultaneous intracellular dye depletion and PI uptake from the extracellular space [10], confirming that the pores were not specific to a particular molecule and transport was driven by the concentration gradient across the pore.

Intracellular transport & kinetics

Therapeutic agents have to overcome various diffusive and metabolic barriers to achieve eventual success. After agents are delivered into the cells via sonoporation, they need to move through the interior of the cell to interact with organelles or other molecular targets to generate their therapeutic effect. For example, in applications using sonoporation to enhance nonviral gene delivery to cells, the therapeutic agent or vector (e.g., plasmid DNA) must transport through the cytoplasm after internalization and enter the nucleus for successful gene expression.

Cytoplasmic transport after uptake through plasma membrane pores

As an example of intracellular transport, consider the sonoporation-mediated delivery of plasmid DNA in nonviral gene transfection [77]. In this study, plasmid delivery was generally enhanced by the simultaneous use of pulsed ultrasound with microbubbles. For direct observation of intracellular kinetics, plasmid DNA can be labeled using fluorescent intercalating agents. In contrast to **lipofection**, sonoporation results in a more homogenous distribution of plasmid DNAs into the cell cytoplasm (Figure 6) [54,78–79]. Protein expression of the introduced DNA was also much faster for sonoporation (reaching maximum at 5–6 h after ultrasound application) than for lipofection (reaching maximum after ~24 h) [78]. Moreover, the fluorescence signal diminished much faster after ultrasound

application (within ~4–8 h) than after lipofection (>24 h) [54]. The rapid decrease of fluorescence after sonoporation is likely the result of degradation of unprotected plasmid DNAs by intracellular DNases, indicating possible challenges of nonviral gene delivery to achieve high level of transfection.

One TEM study has suggested that sonicated cells (both with and without microbubbles) showed chromatin condensation in the nucleus in some cases and a lightened appearance of the cytoplasm, suggesting a loss of cytoplasm viscosity, which could affect the rate of intracellular transport of delivered agents [61]. More investigation is needed to elucidate the entire process of therapeutic agents inside the cell, so that strategies can be developed to improve the fate of these agents.

Nuclear membrane transport & gene expression

Small molecules (≤40 kDa) can diffuse through nuclear pores, but larger molecules such as plasmid DNA may not be easily transported across the nuclear envelope efficiently by passive diffusion due to restriction of the nuclear pore complex [80]. Interestingly, it has been observed that plasmid DNA appeared inside the nucleus after extended (up to 30 min) exposure to pulsed ultrasound [62,81], suggesting that transfection enhancement occurred because either more cells were sonoporated and/or more plasmids were delivered to the cells. However, in general, it has been challenging for nonviral methods to achieve efficient gene transfection due to factors such as intracellular degradation of DNA and limited nuclear transport.

A recent study reported experiments that first internalized plasmid DNA to the intracellular space using calcium phosphate co-precipitates (‘calfection’ [82]), and then used ultrasound to significantly enhance transfection of the plasmids already existing inside the cells [83]. As the nuclear pore complex is controlled in part by Ca^{2+} and ultrasound exposure is known to affect the calcium ion concentration in the cell [73] (see further discussion in the section “Change of intracellular calcium ion concentration”), ultrasound may be indirectly inducing the enhanced uptake to the nucleus. As microbubbles were not present inside the cytoplasm, additional work is needed to elucidate the detailed mechanisms involved in ultrasound-enhanced gene delivery, which is dependent on multiple processes from uptake to eventual gene transfection.

Cytoplasmic transport after uptake via endocytosis

Formation of nonspecific pores, or physical disruption in the plasma membrane, may not be the only route for intracellular delivery. It has been reported that endocytosis occurred with ultrasound application at low acoustic pressure (0.22 MPa) and long exposure time (30 s with 6.2% duty cycle, 20 Hz PRF) [76]. This study showed that after ultrasound treatment, 155 kDa and 500 kDa FITC-dextrans were present in distinct vesicles, no uptake of 500 kDa dextran was observed after ATP depletion, and co-localization of 500 kDa dextran with caveolin-1 and clathrin, which are markers for endocytosis (Figure 7A). Another study showed that after sonoporation, fluorescent-labeled plasmid DNA (~4.95 MDa) was localized in individual vesicles and gradually approached the nucleus as time progressed (Figure 7B) [38]. However, whether endocytosis is always involved after sonoporation for

large macromolecules is still under debate. Experiments of ultrasound mediated plasmid delivery (gWiz-GFP; 5757 bp) at a reduced temperature (4°C), which significantly lowered membrane fluidity and the endocytic process, showed sonoporation at slightly reduced levels (5–10%) [78]. In addition, a recent study also showed that ultrasound application did not result in gene expression from a viral vector that can only achieve gene expression via endocytosis, suggesting the absence of endocytosis in these experiments [84]. Thus further study is needed to clarify these important issues relevant to ultrasound-mediated delivery.

Applications of ultrasound mediated drug delivery & gene therapy

A wide range of applications using ultrasound delivery have been reported. Ultrasound has been used to enhance drug and gene delivery in a variety of contexts [38,85–86] with emphasis on delivery to the brain [87,88], cardiovascular system [89,90], and solid tumors [91]. A full discussion of these applications is beyond the scope of this review. Here we aim to describe some recent studies to illustrate successful applications of the technique.

Ultrasound-mediated drug delivery for cancer treatment

One of the major goals of cancer research is to develop more effective drug treatments. The major mechanism of anticancer drugs is to inhibit cell proliferation or promote programmed cell death (apoptosis) of the cancer cells. Anticancer drugs are also often severely toxic to healthy cells. Compared with conventional drug-delivery methods, such as intravenous injection or oral administration, targeted-drug delivery using ultrasound and microbubbles can substantially reduce undesirable systemic side effects. Compared with using the anti-cancer drug bleomycin alone, a combination of ultrasound and microbubbles successfully inhibited cancer cell growth at a much lower dosage, demonstrated by the shrinkage of tumor in an *in vivo* melanoma tumor model in mice [92]. For brain cancer treatment, the intact blood–brain barrier (BBB) often prevents cytotoxic levels of anticancer drugs such as doxorubicin (DOX) from being achieved. Much effort and success have been obtained developing techniques of focused ultrasound application with microbubbles to transient permeate the BBB for targeted-drug delivery [93,94]. Using a MRI-guided ultrasound with microbubbles to locally disrupt the BBB, a therapeutic level of DOX concentration was achieved in brain tissue [95]. To efficiently suppress DOX systemic toxicity, especially in the heart, kidney and liver, DOX-liposome-loaded microbubbles were designed and fabricated for targeted ultrasound mediated local release of DOX to cancer cells without affecting other cells [96]. A recent study focused on ultrasound exposure with microbubbles and magnetic nanoparticles loaded with epirubicin has shown delivery across the BBB [97]. After using an inhomogeneous field to target the nanoparticles to the tumor region in a murine model, the deposition of the nanoparticles in brain tumors with ultrasound treatment showed significant increases in concentration relative to control regions in the contralateral hemisphere.

Ultrasound mediated nonviral gene transfection

Efficient and safe delivery methods for genetic materials has long been a major challenge for gene therapy. Most genetic materials are macromolecules and negatively charged, resulting in difficulty for them to spontaneously transport across the negatively charged,

lipophilic plasma membrane. Viral vectors, based on the naturally evolved ability of viruses to efficiently transfer genetic material into host cells, are superior to their nonviral counterparts in gene transfection [98]. However, the possibility of viral vectors to evoke inflammatory and adverse immunogenic responses has hindered clinical translation [99,100]. Numerous studies have shown the feasibility of ultrasound-and microbubble-mediated gene transfection for nonviral gene delivery with great potential to be a safe alternative of gene transfection [38,86]. For example, a study showed that with ultrasound exposures (1 MHz, 25% duty cycle, 1–4 W/cm^2 intensity) combined with microbubbles, 18% gene transfection efficacy was achieved *in vitro*, and prolonged functional gene expression in mouse hind leg muscle and in tumors was demonstrated *in vivo* [101]. In another study, short antisense androgen receptor oligodeoxynucleotides were loaded on the lipid shell of cationic microbubbles by ion charge binding, and were released into cells by bursting the microbubbles with ultrasound [102]. The study showed that 49% of prostate tumor cells were transfected and showed a decrease in androgen receptor expression compared with untreated control cells, with the result confirmed *in vivo* in a murine model. Another recent study of glioblastoma cells showed a transfection rate of 70% *in vitro* with cell mortality at less than 15% using smaller microbubbles (Vevo Micromarker™; VisualSonics, Amsterdam, The Netherlands), corresponding to a 1.5-fold improvement over larger microbubbles [103].

In addition to facilitated pore opening, microbubbles have also been engineered to serve as gene carriers. For example, one study showed that under ultrasound exposure (1 MHz, 0.3 MPa pressure, 50 cycles), cationic microbubbles, which were electrostatically coupled with plasmid DNA, resulted in approximately 1% gene transfection efficiency to rat vascular smooth muscle cells with 40% viability *in vitro* [5]. We obtained 6.9% gene transfection to the same cell line by employing a novel ultrasound exposure protocol [54]. Multi-functional microbubbles have also been employed, as demonstrated in a study where endothelial-targeted cationic microbubbles carrying cDNA resulted in selective attachment to the microvasculature and successfully achieved gene transfection [6]. Microbubbles bearing a luciferase plasmid, which were molecularly targeted for gut endothelial cell inflammation, resulted in strong ultrasound contrast intensity at the diseased region from accumulated microbubbles, and luciferase expression was detected 48 h later [104].

Bioeffects generated by ultrasound excitation of microbubbles

In addition to the intracellular transport of therapeutic agents across the membrane, ultrasound exposure in the presence of microbubbles can generate bioeffects that may also have important applications. Here we highlight three classes of bioeffects: intracellular calcium changes, apoptosis, and membrane/cytoskeletal changes.

Change of intracellular calcium ion concentration

The calcium ion plays important roles in regulating many physiological processes, including healing of wounds, controlling the automatic rhythmic contraction of cardiomyocytes, evoking action potential in neurons, and triggering apoptosis [105–107]. Hence, studying the changes in intracellular calcium concentration by ultrasound and microbubbles may be important to gain a complete assessment of the technology [73].

Transient Ca^{2+} influx has been reported in several studies using fluorescence microscopy to investigate cells pre-loaded with calcium-sensitive dyes [40,67,74108–111]. In some cases, change in the intracellular concentration of Ca^{2+} ($[Ca^{2+}]$) occurred immediately after application of the ultrasound exposure. In many cases, the $[Ca^{2+}]$ change was due to influx of Ca^{2+} diffusing through pores into the cells, along with concurrent influx of another cell-impermeant extracellular marker (e.g., PI) [10]. However, in brain endothelial cells, we have also observed that smaller but still significant $[Ca^{2+}]$ increases can occur immediately without any detectable influx of PI, suggesting that the ultrasound application generated: release of intracellular stores such as the endoplasmic reticulum, mitochondria, or buffering proteins; or stretch-activated channels that are specific to Ca^{2+}[110]. Interestingly, when endothelial cells (Bend.3, HUVEC) are cultured in microfluidic channels under the shear stress of continuous fluid flow, the increases of both PI and Ca^{2+} due to ultrasound exposure were reduced compared to cells in static culturing, suggesting a possible adaptive 'hardening' effect under these more realistic conditions [111]. In other cases, $[Ca^{2+}]$ changes, including oscillations, occurred seconds to minutes after ultrasound exposure, revealing the presence of intercellular calcium waves propagating away from cells triggered at the time of ultrasound exposure [74,108]. These ultrasound-induced waves may have resulted from the mechanical stimulation of ultrasound excited bubbles, as in direct mechanical contact and fluid flow, which are mediated by intracellular [112] or extracellular messengers [113].

Ultrasound-induced apoptosis

While ultrasound-induced cavitation can cause various kinds of wounding, which may result in necrosis [114], it also has been shown that apoptosis (programmed cell death) can also be triggered [115]. Components or fragments from apoptotic cells can be cleared by phagocytic cells without causing inflammatory responses or damage to surrounding cells. Using ultrasound to achieve controlled and targeted triggering of apoptosis has the potential to provide an efficient way to treat cancer, by inducing death of the rapidly proliferating cancer cells via the apoptotic pathway.

Cell changes associated with apoptosis such as cell shrinkage, cell membrane roughening/ruffling, appearance of vacuoles and blebs, nuclear fragmentation, and DNA fragmentation have been observed after ultrasound treatment in the presence of microbubbles [116–120]. This apoptosis has been attributed to a generation of free radicals [116] and reactive oxygen species [117], the influx of Ca^{2+} [117], and undetermined sonomechanical effects [118]. A recent study of leukemia cells has indicated that sonoporation of resealed viable cells can result in cleavage of certain proteins that affect DNA repair functionality and can interfere with mitochondrial signaling pathways that affect the cell-cycle progression, thereby increasing the likelihood of apoptosis [119]. We have demonstrated that it is possible to cause localized cell death that is primarily apoptotic within a larger cell population using an aqueous two-phase system to targeted microbubbles of selected areas on a cell culture [120]. The ultrasound-induced apoptosis increased with higher extracellular $[Ca^{2+}]$, with cells showing characteristic apoptotic responses including loss of mitochondrial membrane potential, caspase activation, and changes in nuclear morphology. The opposite condition of

targeted calcium chelation after sonication has been shown to significantly reduce the incidence of apoptosis [115].

Changes in transmembrane potential & cytoskeleton

Both fluorescence microscopy using the voltage sensitive dye (di-4-ANEPPs) [121] and the whole-cell current clamp technique have indicated that hyperpolarization of the cell membrane occurred during ultrasound exposure of cells in the vicinity of microbubbles [122–124]. Activation of BK_{Ca} channels has been suggested to be the cause of the hyperpolarization. Such changes of transmembrane potential of the cells due to ultrasound application might affect the ion transport in the cells, which in turn can affect cellular function. These observations may be particularly relevant for excitable cells such as myocytes and neurons, although the mechanisms of ultrasound-induced excitation of neuronal cells are still under investigation [97].

Ultrasound exposures have also been shown to generate changes in cytoskeletal F-actin stress fibers. Transient increase and rearrangement after ultrasound exposure without microbubbles have been observed, with enhanced effects in the presence of microbubbles [109]. Since the low diffusion coefficient of large DNA molecules in the cytoplasm may severely limit the ability of these molecules to reach the nucleus [125], there is an intriguing possibility of using ultrasound to induce changes of the cytoskeleton, either to transiently increase the apparent diffusion coefficient or to even induce the active transport machinery of the cells to increase ultrasound-mediated gene transfection efficiency.

Ultrasound-mediated cytoskeleton rearrangement has attracted increasing attention for various applications, including tissue engineering and mechano-transduction applications. For example, a recent study reported significant effects of ultrasound stimulation on the cytoskeleton organization of chondrocytes in a 3D matrix [126]. In our recent study, we used ultrasound pulses and targeted microbubbles to exert mechanical stimulations on a subcellular area where the microbubble was attached to the cell. The force exerted by the ultrasound on the microbubble subsequently lead to intracellular cytoskeleton contractility enhancement. Our results demonstrated that this ‘ultrasound tweezing cytometry’ has a great potential for biomechanical stimulation of cells [127].

Challenges & limitations

The noninvasive nature, low toxicity, targeted and local application, versatility, cost-effectiveness, and potential to achieve imaging-guided therapy are significant advantages of ultrasound-mediated delivery with microbubbles. However, important challenges still face its application, including relatively low delivery efficiency and variation in delivery outcomes compared with viral vectors or nonvirus counterparts, such as lipofection and electroporation [78,120,128].

Ultrasound-mediated delivery facilitated by microbubbles is a complex, multistep process, involving the physical process of ultrasound-excited microbubbles and their interaction with the cells, the internalization of the therapeutic agents either from diffusion or endocytosis, the biochemical processes in cytoplasm, and the drug activation or gene expression. While

great progress has been made in understanding each of the steps in the process, the complete mechanism remains to be clearly elucidated. Optimization of outcome has largely relied on empirical approaches [57,129130] and there is a lack of rational design, which is dependent on improved understanding of the underlying mechanisms.

Pore size may be a limiting factor hindering the transport of therapeutic agents across the cell membrane, especially macromolecules, such as plasmid DNA. Plasmid DNA usually has a molecular weight on the order of MDa, and its diameter is on the 100 nm scale [131]. Electrophysiology measurement and postultrasound microscopic images of fixed cells have shown that disruptions on cell membrane can generate pores with a diameter from several nanometers to several 100 nm [8–9,40,60,63]. However, it has not been clearly demonstrated whether the large pore size generated by ultrasound exposure will induce cell death or alter cell functions affecting successful gene expression, as these larger pores on cell membrane may compromise cell viability. It is also unclear what percentage or types of cells can sustain pores larger than 100 nm. Our recent study found that the percentage of pores with diameters larger than 25 nm increased from 5.0 to 16.4 to 29.3% as more powerful ultrasound stimulations were applied, while the cell viability decreased from 94.6 to 72.0 to 62.2%, respectively [120].

Depending on ultrasound conditions, two routes have been suggested for internalization of therapeutic agents into cells: physical pores and endocytosis. If the agent (plasmid DNA or other large molecules) enter the cytoplasm through pores, some protective measures against natural metabolism (e.g., DNase hydrolysis) and/or strategies for facilitating the transport the agent to its target destination may increase the agent's efficacy. If endocytosis is involved, methods to protect the agent against the acidic environment in the late endosomes and the lysosomes, or methods to promote escape from the endosome, could help to improve efficacy. In general, ultrasound-mediated gene transfection faces similar challenges as other nonviral strategies with limited transfection efficiency. Much effort is needed to overcome this difficulty in order to develop the ultrasound technique as a viable clinical technique.

Future perspective

While much has been learned about how ultrasound can induce microbubble-facilitated sonoporation, future development of the field will depend on additional research to translate the insights gained from controlled laboratory experiments to clinical application. For example, more studies will need to be performed under conditions more similar to the environment *in vivo*. Geometric configurations of microbubbles with regard to cells, the effects of culturing conditions (e.g., fluid stresses, 3D arrangement, chemical environments), and effects of ultrasound on delivery in cells in 3D or bulk tissue will all be important factors to consider. In addition, a more detailed mechanistic understanding of the bioeffects of ultrasound on cell organelles and cell's internal environment, and the longer term effects on cell reproduction and growth, will be important and useful to understand the safety of the technique. For example, a recent study of cells *in vitro* has confirmed that while low intensities of ultrasound (<0.1 W/cm^2) were safe, intermediate intensities of ultrasound (0.3–0.4 W/cm^2) can give rise to a genotoxicity (DNA double-strand breaks) of comparable magnitude to ionizing radiation, suggesting dose studies should be performed to minimize

such undesirable side effects *in vivo* [132]. We expect that the trend to develop targeted microbubbles for visualizing the molecular markers of disease, such as thrombosis, inflammation, ischemia/reperfusion injury, angiogenesis and related conditions will continue [17,133]. Moreover, microbubbles will continue to be engineered as vehicles to carry therapeutic payloads, such as DNA [5,6], thereby giving rise to an increasingly large class of hybrid 'theranostic' agents. However, many questions and challenges remain in this regard. For example, will microbubbles be able to carry sufficient amount of payload? Will the payload be able to be released from microbubbles without damage to the payload and nearby tissue? Will there be any effects on the physiochemical properties of the therapeutic payload by the high temperature and pressure induced by inertial cavitation? Further studies will be required to address all of these questions while continuing to study the efficacy and safety of ultrasound-mediated drug and gene delivery. Although much work lies ahead, ultrasound-mediated delivery facilitated by microbubbles presents a promising and attractive strategy for *in vivo* applications, leveraging the advantages of affordable and worldwide nature of ultrasound technology.

Acknowledgments

The authors thank GL Ryan for helpful comments on a draft version of the manuscript.

Keyterms

Microbubble	Micrometer-size gas-filled cavity; modern versions are typically encapsulated microspheres with a radius of 0.5–3.5 μm, a water-insoluble gas core (such as a perfluorocarbon gas), and a stabilizing thin (nm) shell. Targeted microbubbles have special coatings that allow the microbubbles to attach to cells via chemical ligands (e.g., avidin–biotin binding)
Ultrasound	Wave of pressure (or density) changes at frequencies above the range of human hearing, typically more than 20 kHz, but often more than 1 MHz in clinical systems for imaging and therapy
Sonoporation	Transient and reversible increase in cell membrane permeability usually due to membrane disruption induced by ultrasound, often in conjunction with microbubbles
Cavitation	Inception or response of gaseous cavities (bubbles) by ultrasound, stable cavitation describes the periodic volume expansion and contraction of microbubbles without destruction, while transient (inertial) cavitation occurs when the bubble rapidly expands to more than twice of its preultrasound radius followed by collapse driven by the inertia of surrounding fluid
Microstreaming	Bulk motion of fluid caused by cavitation of a microbubble under the influence of ultrasound exposure

Acoustic radiation force	Net forces generated by an ultrasound field. Primary acoustic radiation force is associated with the incident ultrasound field and can cause translation of microbubbles; secondary acoustic radiation force is generated by scattering by the microbubbles in the primary incident ultrasound field. Secondary acoustic radiation force is often attractive among bubbles and can lead to microbubble aggregation or coalescence
Lipofection	Method of introducing genetic material into a cell by means of vesicles (liposomes) consisting of a phospholipid bilayer that can easily merge with the cell membrane; often used for *in vitro* gene transfection.

References

Papers of special note have been highlighted as:

• of interest.

1. Klibanov AL. Microbubble contrast agents: targeted ultrasound imaging and ultrasound-assisted drug-delivery applications. Invest Radiol. 2006; 41(3):354–362. [PubMed: 16481920]
2. Kaufmann BA, Lindner JR. Molecular imaging with targeted contrast ultrasound. Curr Opin Biotechnol. 2007; 18(1):11–16. [PubMed: 17241779]
3. Price RJ, Skyba DM, Kaul S, Skalak TC. Delivery of colloidal particles and red blood cells to tissue through microvessel ruptures created by targeted microbubble destruction with ultrasound. Circulation. 1998; 98(13):1264–1267. [PubMed: 9751673]
4. Miller DL, Quddus J. Sonoporation of monolayer cells by diagnostic ultrasound activation of contrast-agent gas bodies. Ultrasound Med Biol. 2000; 26(4):661–667. [PubMed: 10856630]
5. Phillips LC, Klibanov AL, Wamhoff BR, Hossack JA. Targeted gene transfection from microbubbles into vascular smooth muscle cells using focused, ultrasound-mediated delivery. Ultrasound Med Biol. 2010; 36(9):1470–1480. [PubMed: 20800174]
6. Xie A, Belcik T, Qi Y, et al. Ultrasound-mediated vascular gene transfection by cavitation of endothelial-targeted cationic microbubbles. JACC Cardiovasc Imaging. 2012; 5(12):1253–1262. [PubMed: 23236976]
7. Husseini GA, Pitt WG. Micelles and nanoparticles for ultrasonic drug and gene delivery. Adv Drug Deliv Rev. 2008; 60(10):1137–1152. [PubMed: 18486269]
8•. Prentice P, Cuschieri A, Dholakia K, Prausnitz M, Campbell P. Membrane disruption by optically controlled microbubble cavitation. Nat Phy. 2005; 1(2):107. Uses high-speed video microscopy and optical trapping of microbubbles to clearly demonstrate microbubble collapse can result in jetting and formation in cells.
9•. Schlicher RK, Radhakrishna H, Tolentino TP, Apkarian RP, Zarnitsyn V, Prausnitz MR. Mechanism of intracellular delivery by acoustic cavitation. Ultrasound Med Biol. 2006; 32(6): 915–924. Demonstrates that cavitation induces uptake of macromolecules using flow cytometry, electron microscopy, and fluorescence microscopy and images showing membrane repair after sonporation. [PubMed: 16785013]
10. Fan Z, Kumon RE, Park J, Deng CX. Intracellular delivery and calcium transients generated in sonoporation facilitated by microbubbles. J Control Release. 2010; 142(1):31–39. [PubMed: 19818371]
11. Leighton, TG. The Acoustic Bubble. Academic Press; San Diego, CA, USA: 1994.
12. Qin S, Caskey CF, Ferrara KW. Ultrasound contrast microbubbles in imaging and therapy: physical principles and engineering. Phys Med Biol. 2009; 54(6):R27–R57. [PubMed: 19229096]

13. Ferrara K, Pollard R, Borden M. Ultrasound microbubble contrast agents: Fundamentals and application to gene and drug delivery. Annu Rev Biomed Eng. 2007; 9:415–447. [PubMed: 17651012]
14. Kaul S. Myocardial contrast echocardiography: a 25-year retrospective. Circulation. 2008; 118(3): 291–308. [PubMed: 18625905]
15. Borden MA, Longo M. Dissolution behavior of lipid monolayer-coated, air-filled microbubbles: effect of lipid hydrophobic chain length. Langmuir. 2002; 18:9225–9233.
16. Goertz DE, De Jong N, Van der Steen AF. Attenuation and size distribution measurements of Definity and manipulated Definity populations. Ultrasound Med Biol. 2007; 33(9):1376–1388. [PubMed: 17521801]
17. Klibanov AL. Preparation of targeted microbubbles: ultrasound contrast agents for molecular imaging. Med Biol Eng Comput. 2009; 47(8):875–882. [PubMed: 19517153]
18. Ferrara KW, Borden MA, Zhang H. Lipid-shelled vehicles: engineering for ultrasound molecular imaging and drug delivery. Acc Chem Res. 2009; 42(7):881–892. [PubMed: 19552457]
19. Delalande A, Kotopoulis S, Rovers T, Pichon C, Postema M. Sonoporation at a low mechanical indiex. Bubble Sci Engin Technol. 2011; 3:3–11.
20. Marmottant P, Hilgenfeldt S. Controlled vesicle deformation and lysis by single oscillating bubbles. Nature. 2003; 423(6936):153–156. [PubMed: 12736680]
21. Longuet-Higgins MS. Viscous streaming from an oscillating spherical bubble. Proc R Soc London A. 1998; 454:725–742.
22. Wu J. Shear stress in cells generated by ultrasound. Prog Biophys Mol Biol. 2007; 93(1–3):363–373. [PubMed: 16928394]
23. Van Bavel E. Effects of shear stress on endothelial cells: possible relevance for ultrasound applications. Prog Biophys Mol Biol. 2007; 93(1–3):374–383. [PubMed: 16970981]
24. Crum LA, Roy RA. Sonoluminescence. Science. 1994; 266(5183):233–234. [PubMed: 17771441]
25. Miller DL, Thomas RM. Ultrasound contrast agents nucleate inertial cavitation *in vitro*. Ultrasound Med Biol. 1995; 21(8):1059–1065. [PubMed: 8553500]
26. Miller MW, Miller DL, Brayman AA. A review of *in vitro* bioeffects of inertial ultrasonic cavitation from a mechanistic perspective. Ultrasound Med Biol. 1996; 22(9):1131–1154. [PubMed: 9123638]
27. Lauterborn W, Ohl CD. Cavitation bubble dynamics. Ultrason Sonochem. 1997; 4(2):65–75. [PubMed: 11237047]
28. Sundaram J, Mellein BR, Mitragotri S. An experimental and theoretical analysis of ultrasound-induced permeabilization of cell membranes. Biophys J. 2003; 84(5):3087–3101. [PubMed: 12719239]
29. Hallow DM, Mahajan AD, McCutchen TE, Prausnitz MR. Measurement and correlation of acoustic cavitation with cellular bioeffects. Ultrasound Med Biol. 2006; 32(7):1111–1122. [PubMed: 16829325]
30. Zhou Y, Cui J, Deng CX. Dynamics of sonoporation correlated with acoustic cavitation activities. Biophys J. 2008; 94(7):L51–53. [PubMed: 18212008]
31. Husseini GA, Diaz de la Rosa MA, Richardson ES, Christensen DA, Pitt WG. The role of cavitation in acoustically activated drug delivery. J Control Release. 2005; 107(2):253–261. [PubMed: 16046023]
32. Benjamin TB, Ellis AT. The collapse of cavitation bubbles and the pressures thereby produced against solid boundaries. Phil Trans Roy Soc. 1966; A260:221–240.
33. Lauterborn W, Bolle H. Experimental investigation of cavitation-bubble collapse in the neighbourhood of a solid boundary. J Fluid Mech. 1975; 72:391–399.
34. Prosperetti A. Bubble phenomena in sound fields: part 2. Ultrasonics. 1984; 22:115–124.
35. Plesset MS, Chapman RB. Collapse of an initially spherical vapour cavity in the neighbourhood of a solid boundary. J Fluid Mech. 1971; 47:283–290.
36. Tomita Y, Shima A. Mechanisms of impulsive pressure generation and damage pit formation by bubble collapse. J Fluid Mech. 1986; 169:535–564.

37. Postema M, Kotopoulis S, Delalande A, Gilja OH. Sonoporation: Why microbubbles create pores. Ultraschall Med. 2012; 33(1):97–98.

38. Delalande A, Kotopoulis S, Postema M, Midoux P, Pichon C. Sonoporation: Mechanistic insights and ongoing challenges for gene transfer. Gene. 2013; 525(2):191–199. [PubMed: 23566843]

39. Okada K, Kudo N, Niwa K, Yamamoto K. A basic study on sonoporation with microbubbles exposed to pulsed ultrasound. J Med Ultrasonics. 2005; 32:3–11.

40. Kudo N, Okada K, Yamamoto K. Sonoporation by single-shot pulsed ultrasound with microbubbles adjacent to cells. Biophys J. 2009; 96(12):4866–4876. [PubMed: 19527645]

41•. Van Wamel A, Kooiman K, Harteveld M, et al. Vibrating microbubbles poking individual cells: drug transfer into cells via sonoporation. J Control Release. 2006; 112(2):149–155. Uses high-speed microscopy to show that stable cavitation of microbubbles can result in cell deformation that is related to transient increases in cell permeability shown by a fluorescent marker. [PubMed: 16556469]

42. Kooiman K, Foppen-Harteveld M, Van Der Steen AF, De Jong N. Sonoporation of endothelial cells by vibrating targeted microbubbles. J Control Release. 2011; 154(1):35–41. [PubMed: 21514333]

43. Forbes MM, Steinberg RL, O'Brien WD Jr. Examination of inertial cavitation of Optison in producing sonoporation of chinese hamster ovary cells. Ultrasound Med Biol. 2008; 34(12):2009–2018. [PubMed: 18692296]

44. Forbes MM, Steinberg RL, O'Brien WD Jr. Frequency-dependent evaluation of the role of Definity in producing sonoporation of Chinese hamster ovary cells. J Ultrasound Med. 2011; 30(1):61–69. [PubMed: 21193706]

45. Forbes MM, O'Brien WD Jr. Development of a theoretical model describing sonoporation activity of cells exposed to ultrasound in the presence of contrast agents. J Acoust Soc Am. 2012; 131(4): 2723–2729. [PubMed: 22501051]

46. Krasovitski B, Frenkel V, Shoham S, Kimmel E. Intramembrane cavitation as a unifying mechanism for ultrasound-induced bioeffects. Proc Natl Acad Sci USA. 2011; 108(8):3258–3263. [PubMed: 21300891]

47. Zhou Y, Yang K, Cui J, Ye JY, Deng CX. Controlled permeation of cell membrane by single bubble acoustic cavitation. J Control Release. 2012; 157(1):103–111. [PubMed: 21945682]

48. Dayton P, Klibanov A, Brandenburger G, Ferrara K. Acoustic radiation force *in vivo*: a mechanism to assist targeting of microbubbles. Ultrasound Med Biol. 1999; 25(8):1195–1201. [PubMed: 10576262]

49. Lum AF, Borden MA, Dayton PA, Kruse DE, Simon SI, Ferrara KW. Ultrasound radiation force enables targeted deposition of model drug carriers loaded on microbubbles. J Control Release. 2006; 111(1–2):128–134. [PubMed: 16380187]

50. Garbin V, Overvelde M, Dollet B, de Jong N, Lohse D, Versluis M. Unbinding of targeted ultrasound contrast agent microbubbles by secondary acoustic forces. Phys Med Biol. 2011; 56(19):6161–6177. [PubMed: 21878709]

51. Postema M, Marmottant P, Lancee CT, Hilgenfeldt S, de Jong N. Ultrasound-induced microbubble coalescence. Ultrasound Med Biol. 2004; 30(10):1337–1344. [PubMed: 15582233]

52. Kokhuis TJ, Garbin V, Kooiman K, et al. Secondary Bjerknes forces deform targeted microbubbles. Ultrasound Med Biol. 2013; 39(3):490–506. [PubMed: 23347643]

53. Mannaris C, Averkiou MA. Investigation of microbubble response to long pulses used in ultrasound-enhanced drug delivery. Ultrasound Med Biol. 2012; 38(4):681–691. [PubMed: 22341047]

54. Fan Z, Chen D, Deng CX. Improving ultrasound gene transfection efficiency by controlling ultrasound excitation of microbubbles. J Control Release. 2013; 170(3):401–413. [PubMed: 23770009]

55. Lawrie A, Brisken AF, Francis SE, Cumberland DC, Crossman DC, Newman CM. Microbubble-enhanced ultrasound for vascular gene delivery. Gene Ther. 2000; 7(23):2023–2027. [PubMed: 11175314]

56•. Mehier-Humbert S, Bettinger T, Yan F, Guy RH. Plasma membrane poration induced by ultrasound exposure: Implication for drug delivery. J Control Release. 2005; 104(1):213–222.

Uses scanning electron microscopy imaging to direct evidence for pore formation on cells resulting from ultrasound treatment with microbubbles. [PubMed: 15866347]

57. Karshafian R, Bevan PD, Williams R, Samac S, Burns PN. Sonoporation by ultrasound-activated microbubble contrast agents: effect of acoustic exposure parameters on cell membrane permeability and cell viability. Ultrasound Med Biol. 2009; 35(5):847–860. [PubMed: 19110370]
58. Chen H, Brayman AA, Kreider W, Bailey MR, Matula TJ. Observations of translation and jetting of ultrasound-activated microbubbles in mesenteric microvessels. Ultrasound Med Biol. 2011; 37(12):2139–2148. [PubMed: 22036639]
59. Tachibana K, Uchida T, Ogawa K, Yamashita N, Tamura K. Induction of cell-membrane porosity by ultrasound. Lancet. 1999; 353(9162):1409. [PubMed: 10227224]
60. Ohl CD, Arora M, Ikink R, et al. Sonoporation from jetting cavitation bubbles. Biophys J. 2006; 91(11):4285–4295. [PubMed: 16950843]
61. Zeghimi A, Uzbekov R, Arbeille B, Escoffre JM, Bouakaz A. Ultrastuctural modifications of cell membranes and organelles induced by sonoporation. IEEE Int Ultrason Symp. 2012:2045–2048.
62. Duvshani-Eshet M, Baruch L, Kesselman E, Shimoni E, Machluf M. Therapeutic ultrasound-mediated DNA to cell and nucleus: bioeffects revealed by confocal and atomic force microscopy. Gene Ther. 2006; 13(2):163–172. [PubMed: 16177822]
63. Zhao YZ, Luo YK, Lu CT, et al. Phospholipids-based microbubbles sonoporation pore size and reseal of cell membrane cultured *in vitro*. J Drug Target. 2008; 16(1):18–25. [PubMed: 18172816]
64. Yang F, Gu N, Chen D, et al. Experimental study on cell self-sealing during sonoporation. J Control Release. 2008; 131(3):205–210. [PubMed: 18727944]
65. Zarnitsyn V, Rostad CA, Prausnitz MR. Modeling transmembrane transport through cell membrane wounds created by acoustic cavitation. Biophys J. 2008; 95(9):4124–4138. [PubMed: 18676653]
66. Zhou Y, Kumon RE, Cui J, Deng CX. The size of sonoporation pores on the cell membrane. Ultrasound Med Biol. 2009; 35(10):1756–1760. [PubMed: 19647924]
67•. Fan Z, Liu H, Mayer M, Deng CX. Spatiotemporally controlled single cell sonoporation. Proc Natl Acad Sci USA. 2012; 109(41):16486–16491. Uses an electrophysiological method (patch-clamp) and fluorescence imaging of a marker dye simultaneously to measure sonoporation of an individual cell by a single bubble in real time. [PubMed: 23012425]
8. Deng CX, Sieling F, Pan H, Cui J. Ultrasound-induced cell membrane porosity. Ultrasound Med Biol. 2004; 30(4):519–526. [PubMed: 15121254]
69. Pan H, Zhou Y, Izadnegahdar O, Cui J, Deng CX. Study of sonoporation dynamics affected by ultrasound duty cycle. Ultrasound Med Biol. 2005; 31(6):849–856. [PubMed: 15936500]
70. Zhou Y, Shi J, Cui J, Deng CX. Effects of extracellular calcium on cell membrane resealing in sonoporation. J Control Release. 2008; 126(1):34–43. [PubMed: 18158198]
71. McNeil PL, Miyake K, Vogel SS. The endomembrane requirement for cell surface repair. Proc Natl Acad Sci USA. 2003; 100(8):4592–4597. [PubMed: 12672953]
72. McNeil PL, Kirchhausen T. An emergency response team for membrane repair. Nat Rev Mol Cell Biol. 2005; 6(6):499–505. [PubMed: 15928713]
73•. Hassan MA, Campbell P, Kondo T. The role of Ca^{2+} in ultrasound-elicited bioeffects: progress, perspectives and prospects. Drug Discov Today. 2010; 15(21–22):892–906. Provides a critical review of the literature regarding ultrasound-induced calcium transients and other bioeffects. [PubMed: 20727981]
74. Kumon RE, Aehle M, Sabens D, et al. Spatiotemporal effects of sonoporation measured by real-time calcium imaging. Ultrasound Med Biol. 2009; 35(3):494–506. [PubMed: 19010589]
75. Guzman HR, Nguyen DX, Mcnamara AJ, Prausnitz MR. Equilibrium loading of cells with macromolecules by ultrasound: effects of molecular size and acoustic energy. J Pharm Sci. 2002; 91(7):1693–1701. [PubMed: 12115831]
76•. Meijering BD, Juffermans LJ, Van Wamel A. Ultrasound and microbubble-targeted delivery of macromolecules is regulated by induction of endocytosis and pore formation. Circ Res. 2009; 104(5):679–687. Provides compelling evidence showing that ultrasound exposure in the presence of microbubbles can endocytosis of macromolecules. [PubMed: 19168443]

77. Duvshani-Eshet M, Adam D, Machluf M. The effects of albumin-coated microbubbles in DNA delivery mediated by therapeutic ultrasound. J Control Release. 2006; 112(2):156–166. [PubMed: 16632040]
78. Mehier-Humbert S, Bettinger T, Yan F, Guy RH. Ultrasound-mediated gene delivery: Kinetics of plasmid internalization and gene expression. J Control Release. 2005; 104(1):203–211. [PubMed: 15866346]
79. Tlaxca JL, Anderson CR, Klibanov AL, et al. Analysis of *in vitro* transfection by sonoporation using cationic and neutral microbubbles. Ultrasound Med Biol. 2010; 36(11):1907–1918. [PubMed: 20800945]
80. Escoffre JM, Teissie J, Rols MP. Gene transfer: how can the biological barriers be overcome? J Membr Biol. 2010; 236(1):61–74. [PubMed: 20623114]
81. Duvshani-Eshet M, Machluf M. Therapeutic ultrasound optimization for gene delivery: a key factor achieving nuclear DNA localization. J Control Release. 2005; 108(2–3):513–528. [PubMed: 16243409]
82. Lindell J, Girard P, Muller N, Jordan M, Wurm F. Calfection: a novel gene transfer method for suspension cells. Biochim Biophys Acta. 2004; 1676(2):155–161. [PubMed: 14746910]
83. Hassan MA, Ahmed IS, Campbell P, Kondo T. Enhanced gene transfection using calcium phosphate co-precipitates and low-intensity pulsed ultrasound. Eur J Pharm Sci. 2012; 47(4):768–773. [PubMed: 22921720]
84. Geers B, Lentacker I, Alonso A, et al. Elucidating the mechanisms behind sonoporation with adeno-associated virus-loaded microbubbles. Mol Pharm. 2011; 8(6):2244–2251. [PubMed: 22014166]
85. Yudina A, Moonen C. Ultrasound-induced cell permeabilisation and hyperthermia: strategies for local delivery of compounds with intracellular mode of action. Int J Hyperthermia. 2012; 28(4): 311–319. [PubMed: 22621733]
86. Escoffre JM, Zeghimi A, Novell A, Bouakaz A. *In vivo* gene delivery by sonoporation: recent progress and prospects. Curr Gene Ther. 2013; 13(1):2–14. [PubMed: 23157546]
87. Deng CX. Targeted drug delivery across the blood-brain barrier using ultrasound technique. Ther Deliv. 2010; 1(6):819–848. [PubMed: 21785679]
88. Burgess A, Hynynen K. Noninvasive and targeted drug delivery to the brain using focused ultrasound. ACS Chem Neurosci. 2013; 4(4):519–526. [PubMed: 23379618]
89. Mayer CR, Bekeredjian R. Ultrasonic gene and drug delivery to the cardiovascular system. Adv Drug Deliv Rev. 2008; 60(10):1177–1192. [PubMed: 18474407]
90. Meairs S, Kern R, Alonso A. Why and how do microbubbles enhance the effectiveness of diagnostic and therapeutic interventions in cerebrovascular disease? Curr Pharm Des. 2012; 18(15):2223–2235. [PubMed: 22352776]
91. Frenkel V. Ultrasound mediated delivery of drugs and genes to solid tumors. Adv Drug Deliv Rev. 2008; 60(10):1193–1208. [PubMed: 18474406]
92. Sonoda S, Tachibana K, Uchino E, et al. Inhibition of melanoma by ultrasound-microbubble-aided drug delivery suggests membrane permeabilization. Cancer Biol Ther. 2007; 6(8):1276–1283. [PubMed: 17704642]
93. Hynynen K, McDannold N, Vykhodtseva N, Jolesz FA. Noninvasive MR imaging-guided focal opening of the blood-brain barrier in rabbits. Radiology. 2001; 220(3):640–646. [PubMed: 11526261]
94. Deng CX, Huang X. Improved outcome of targeted delivery of chemotherapy drugs to the brain using a combined strategy of ultrasound, magnetic targeting and drug-loaded nanoparticles. Ther Deliv. 2011; 2(2):137–141. [PubMed: 22833939]
95. Treat LH, McDannold N, Vykhodtseva N, Zhang Y, Tam K, Hynynen K. Targeted delivery of doxorubicin to the rat brain at therapeutic levels using MRI-guided focused ultrasound. Int J Cancer. 2007; 121(4):901–907. [PubMed: 17437269]
96. Lentacker I, Geers B, Demeester J, De Smedt SC, Sanders NN. Design and evaluation of doxorubicin-containing microbubbles for ultrasound-triggered doxorubicin delivery: cytotoxicity and mechanisms involved. Mol Ther. 2010; 18(1):101–108. [PubMed: 19623162]

97. Liu HL, Hua MY, Yang HW, et al. Magnetic resonance monitoring of focused ultrasound/magnetic nanoparticle targeting delivery of therapeutic agents to the brain. Proc Natl Acad Sci USA. 2010; 107(34):15205–15210. [PubMed: 20696897]

98. Waehler R, Russell SJ, Curiel DT. Engineering targeted viral vectors for gene therapy. Nat Rev Genet. 2007; 8(8):573–587. [PubMed: 17607305]

99. Hartman ZC, Appledorn DM, Amalfitano A. Adenovirus vector induced innate immune responses: impact upon efficacy and toxicity in gene therapy and vaccine applications. Virus Res. 2008; 132(1–2):1–14. [PubMed: 18036698]

100. Nayak S, Herzog RW. Progress and prospects: immune responses to viral vectors. Gene Ther. 2010; 17(3):295–304. [PubMed: 19907498]

101. Li YS, Davidson E, Reid CN, McHale AP. Optimising ultrasound-mediated gene transfer (sonoporation) *in vitro* and prolonged expression of a transgene *in vivo*: potential applications for gene therapy of cancer. Cancer Lett. 2009; 273(1):62–69. [PubMed: 18829156]

102. Haag P, Frauscher F, Gradl J, et al. Microbubble-enhanced ultrasound to deliver an antisense oligodeoxynucleotide targeting the human androgen receptor into prostate tumours. J Steroid Biochem Mol Biol. 2006; 102(1–5):103–113. [PubMed: 17055720]

103. Escoffre JM, Novell A, Piron J, Zeghimi A, Doinikov A, Bouakaz A. Microbubble attenuation and destruction: are they involved in sonoporation efficiency? IEEE Trans Ultrason Ferroelectr Freq Control. 2013; 60(1):46–52. [PubMed: 23287912]

104. Tlaxca JL, Rychak JJ, Ernst PB, et al. Ultrasound-based molecular imaging and specific gene delivery to mesenteric vasculature by endothelial adhesion molecule targeted microbubbles in a mouse model of Crohn's disease. J Control Release. 2013; 165(3):216–225. [PubMed: 23142578]

105. Ghosh A, Greenberg ME. Calcium signaling in neurons: molecular mechanisms and cellular consequences. Science. 1995; 268(5208):239–247. [PubMed: 7716515]

106. Bers DM. Cardiac excitation-contraction coupling. Nature. 2002; 415(6868):198–205. [PubMed: 11805843]

107. Berridge MJ, Bootman MD, Roderick HL. Calcium signalling: dynamics, homeostasis and remodelling. Nat Rev Mol Cell Biol. 2003; 4(7):517–529. [PubMed: 12838335]

108. Kumon RE, Aehle M, Sabens D, Parikh P, Kourennyi D, Deng CX. Ultrasound-induced calcium oscillations and waves in Chinese hamster ovary cells in the presence of microbubbles. Biophys J. 2007; 93(6):L29–31. [PubMed: 17631537]

109. Juffermans LJ, van Dijk A, Jongenelen CA, et al. Ultrasound and microbubble-induced intra- and intercellular bioeffects in primary endothelial cells. Ultrasound Med Biol. 2009; 35(11):1917–1927. [PubMed: 19766381]

110. Park J, Fan Z, Kumon RE, El-Sayed ME, Deng CX. Modulation of intracellular Ca^{2+} concentration in brain microvascular endothelial cells *in vitro* by acoustic cavitation. Ultrasound Med Biol. 2010; 36(7):1176–1187. [PubMed: 20620704]

111. Park J, Fan Z, Deng CX. Effects of shear stress cultivation on cell membrane disruption and intracellular calcium concentration in sonoporation of endothelial cells. J Biomech. 2011; 44(1):164–169. [PubMed: 20863503]

112. Boitano S, Dirksen ER, Sanderson MJ. Intercellular propagation of calcium waves mediated by inositol trisphosphate. Science. 1992; 258(5080):292–295. [PubMed: 1411526]

113. Sauer H, Hescheler J, Wartenberg M. Mechanical strain-induced Ca^{2+} waves are propagated via ATP release and purinergic receptor activation. Am J Physiol Cell Physiol. 2000; 279(2):C295–307. [PubMed: 10912995]

114. Schlicher RK, Hutcheson JD, Radhakrishna H, Apkarian RP, Prausnitz MR. Changes in cell morphology due to plasma membrane wounding by acoustic cavitation. Ultrasound Med Biol. 2010; 36(4):677–692. [PubMed: 20350691]

115. Hutcheson JD, Schlicher RK, Hicks HK, Prausnitz MR. Saving cells from ultrasound-induced apoptosis: quantification of cell death and uptake following sonication and effects of targeted calcium chelation. Ultrasound Med Biol. 2010; 36(6):1008–1021. [PubMed: 20447754]

116. Feril LB Jr, Kondo T, Zhao QL, et al. Enhancement of ultrasound-induced apoptosis and cell lysis by echo-contrast agents. Ultrasound Med Biol. 2003; 29(2):331–337. [PubMed: 12659921]

117. Honda H, Kondo T, Zhao QL, Feril LB Jr, Kitagawa H. Role of intracellular calcium ions and reactive oxygen species in apoptosis induced by ultrasound. Ultrasound Med Biol. 2004; 30(5): 683–692. [PubMed: 15183235]
118. Feril LB Jr, Kondo T, Cui ZG, et al. Apoptosis induced by the sonomechanical effects of low intensity pulsed ultrasound in a human leukemia cell line. Cancer Lett. 2005; 221(2):145–152. [PubMed: 15808400]
119. Zhong W, Sit WH, Wan JM, Yu AC. Sonoporation induces apoptosis and cell cycle arrest in human promyelocytic leukemia cells. Ultrasound Med Biol. 2011; 37(12):2149–2159. [PubMed: 22033133]
120. Frampton JP, Fan Z, Simon A, Chen D, Deng CX, Takayama S. Aqueous two-phase system patterning of microbubbles: Localized induction of apoptosis in sonoporated cells. Adv Funct Mater. 2013; 23:3420–3431.
121. Juffermans LJ, Kamp O, Dijkmans PA, Visser CA, Musters RJ. Low-intensity ultrasound-exposed microbubbles provoke local hyperpolarization of the cell membrane via activation of BK_{Ca} channels. Ultrasound Med Biol. 2008; 34(3):502–508. [PubMed: 17993242]
122. Tran TA, Roger S, Le Guennec JY, Tranquart F, Bouakaz A. Effect of ultrasound-activated microbubbles on the cell electrophysiological properties. Ultrasound Med Biol. 2007; 33(1):158–163. [PubMed: 17189059]
123. Tran TA, Le Guennec JY, Bougnoux P, Tranquart F, Bouakaz A. Characterization of cell membrane response to ultrasound activated microbubbles. IEEE Trans Ultrason Ferroelectr Freq Control. 2008; 55(1):43–49. [PubMed: 18334312]
124. Tran TA, Le Guennec JY, Babuty D, Bougnoux P, Tranquart F, Bouakaz A. On the mechanisms of ultrasound contrast agents-induced arrhythmias. Ultrasound Med Biol. 2009; 35(6):1050–1056. [PubMed: 19195768]
125. Lukacs GL, Haggie P, Seksek O, Lechardeur D, Freedman N, Verkman AS. Size-dependent DNA mobility in cytoplasm and nucleus. J Biol Chem. 2000; 275(3):1625–1629. [PubMed: 10636854]
126. Noriega S, Hasanova G, Subramanian A. The effect of ultrasound stimulation on the cytoskeletal organization of chondrocytes seeded in three-dimensional matrices. Cells Tissues Organs. 2013; 197(1):14–26. [PubMed: 22987069]
127. Fan Z, Sun Y, Di C, et al. Acoustic tweezing cytometry for live-cell subcellular modulation of intracellular cytoskeleton contractility. Sci Rep. 2013; 3:2176. [PubMed: 23846290]
128. Mayer CR, Geis NA, Katus HA, Bekeredjian R. Ultrasound targeted microbubble destruction for drug and gene delivery. Expert Opin Drug Deliv. 2008; 5(10):1121–1138. [PubMed: 18817517]
129. Rahim A, Taylor SL, Bush NL, ter Haar GR, Bamber JC, Porter CD. Physical parameters affecting ultrasound/microbubble-mediated gene delivery efficiency *in vitro*. Ultrasound Med Biol. 2006; 32(8):1269–1279. [PubMed: 16875960]
130. Meijering BD, Henning RH, van Gilst WH, Gavrilovic I, Van Wamel A, Deelman LE. Optimization of ultrasound and microbubbles targeted gene delivery to cultured primary endothelial cells. J Drug Target. 2007; 15(10):664–671. [PubMed: 18041634]
131. Hansma HG, Vesenka J, Siegerist C, et al. Reproducible imaging and dissection of plasmid DNA under liquid with the atomic force microscope. Science. 1992; 256(5060):1180–1184. [PubMed: 1589799]
132. Furusawa Y, Fujiwara Y, Campbell P, et al. DNA double-strand breaks induced by cavitational mechanical effects of ultrasound in cancer cell lines. PLoS ONE. 2012; 7(1):e29012. [PubMed: 22235259]
133. Pysz MA, Gambhir SS, Willmann JK. Molecular imaging: current status and emerging strategies. Clin Radiol. 2010; 65(7):500–516. [PubMed: 20541650]

Executive summary

Microbubbles & sonoporation

- Engineered microbubbles under ultrasound exposure have been used to cause sonoporation and increased permeability of cell membranes to desired agents such as drugs or genes.

Responses of microbubbles to ultrasound excitation

- Shear stresses and microstreaming induced by microbubble oscillation and microjetting induced by microbubble collapse have been proposed as mechanisms for sonoporation.
- Acoustic radiation forces, the choice of ultrasound parameters, and geometrical configuration of an experiment can also affect microbubble response and sonoporation outcomes.

Transient delivery processes across the cell membrane

- Pore size has been estimated from the nanometer to the micrometer range using direct imaging techniques (e.g., scanning electron microscope, transmission electron microscopy, atomic force microscopy), electrophysiological techniques, and fluorescence microscopy.
- Sonoporation typically results in pores that are nonspecific to particular molecules and exhibit bi-directional transport driven by concentration gradients.

Intracellular transport & kinetics

- During gene transfection, sonoporation results in a more homogeneous distribution of plasmid DNAs in the cytoplasm and faster protein expression as compared with lipofection.
- Longer durations of ultrasound exposure may induce endocytosis of large macromolecules.

Applications of ultrasound-mediated drug delivery & gene therapy

- Ultrasound has been shown to improve drug delivery to tumors, cause temporary disruption of the blood–brain barrier, and perform non-viral gene transfection *in vitro* and *in vivo*.

Bioeffects generated by ultrasound excitation of microbubbles

- Ultrasound excitation of microbubbles can cause changes of $[Ca^{2+}]$ in adjacent cells, induce calcium waves in surrounding cells, generate apoptosis, and induce changes in the transmembrane potentialand cellular cytoskeleton.

Challenges & limitations

- More studies are needed to improve delivery efficiency, reduce variation in outcomes, and better understand ultrasound-mediated uptake, transport, and bioeffects.

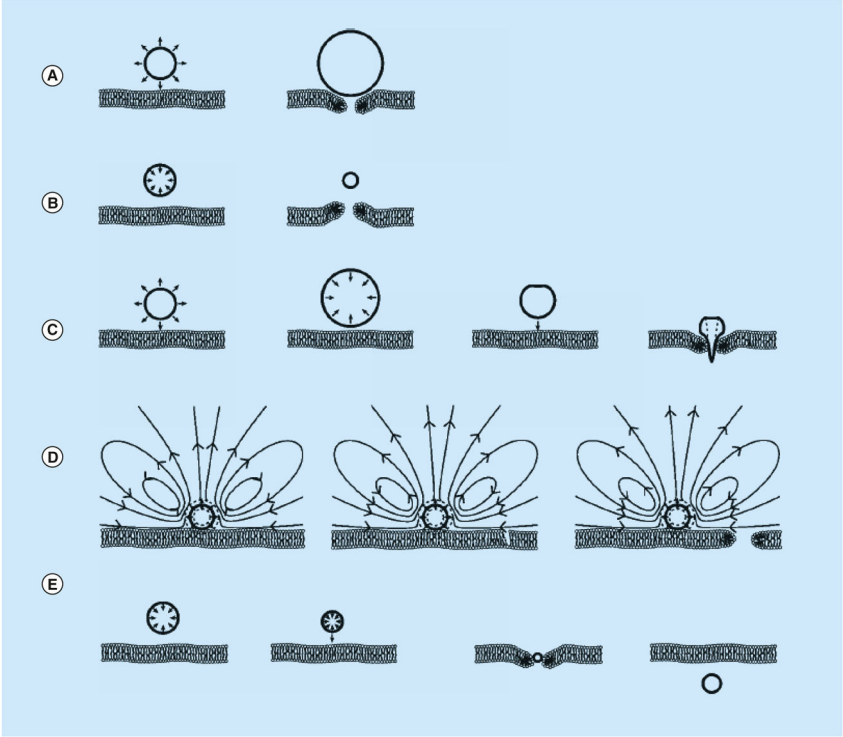

Figure 1. Potential mechanisms for sonoporation

(A) Pushing induced by stable cavitation. **(B)** Pulling induced by stable cavitation. **(C)** Jetting induced by inertial cavitation. **(D)** Microstreaming induced by stable cavitation. **(E)** Translation induced by primary acoustic radiation force.

Reproduced with permission from [19].

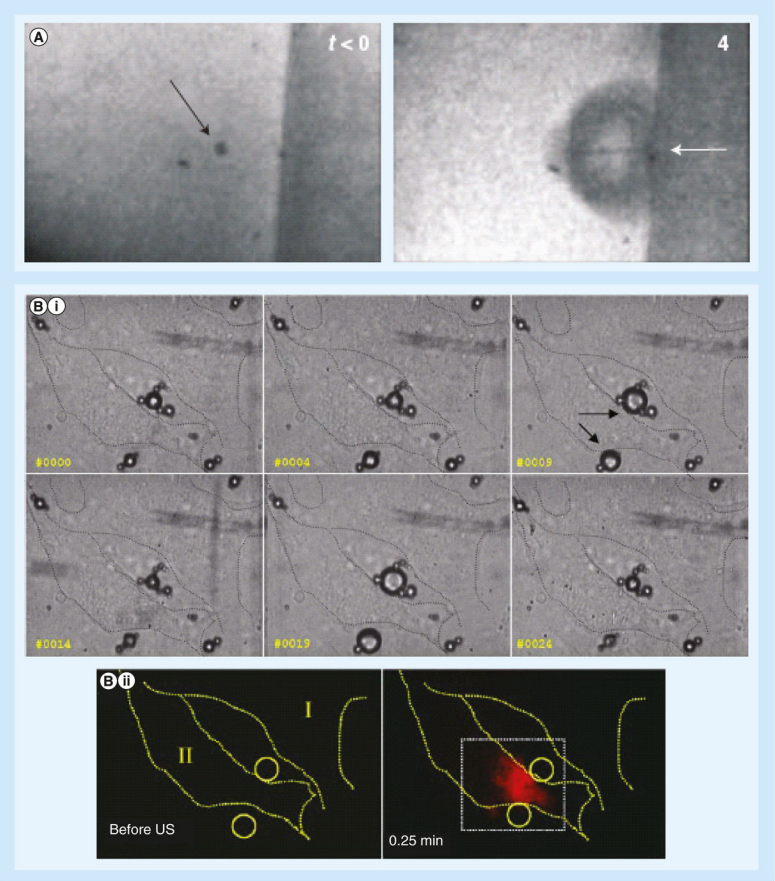

Figure 2. Microbubbles undergo cavitation in contact of cells

(A) Formation of microjet. Before ultrasound exposure (left), the arrow points to a microbubble held in place by an optical trap. During ultrasound exposure (4 μs later; right), the microbubble collapses, and the arrow points to a microjet directed toward the cell attached to the surface on the right. **(B)** Series of high-speed images show **(i)** microbubbles (arrows) experience stable cavitation (oscillations) during ultrasound exposure that **(ii)** led to cellular uptake of the cell impermeable reagent propidium iodide.

US: Ultrasound.

(A) Reproduced with permission from [8]; **(B)** Reproduced with permission from [41].

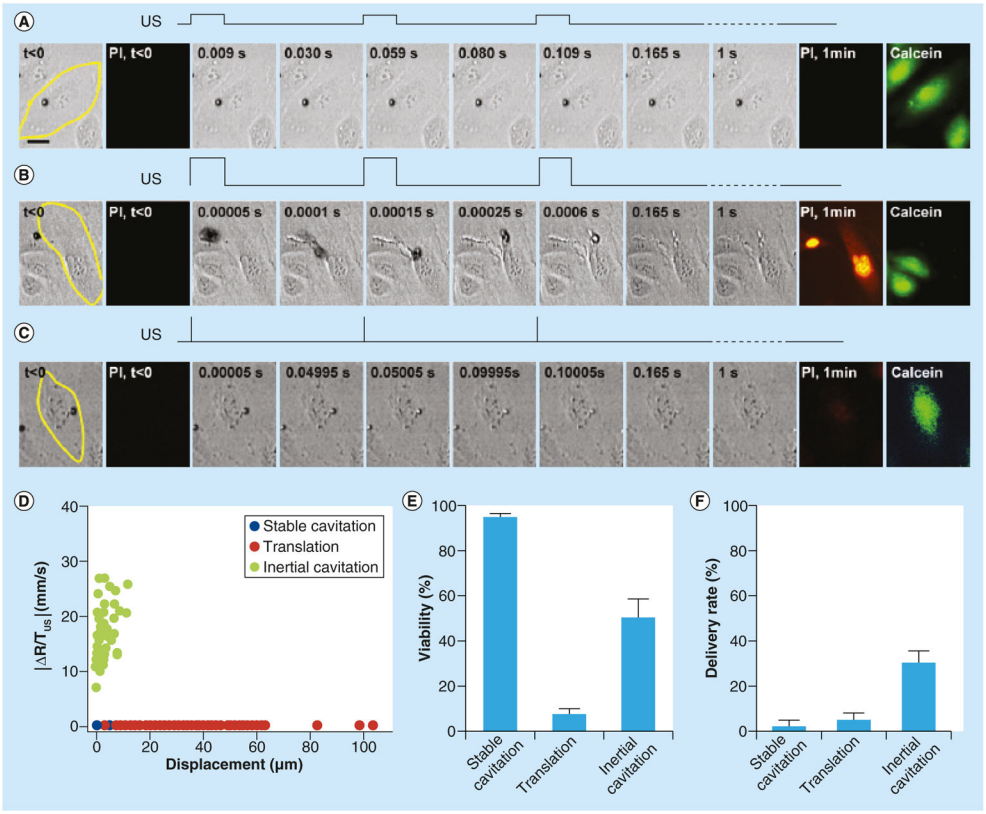

Figure 3. Three typical types of bubble dynamics in application circumstances driven by different ultrasound conditions

These are featured by **(A)** stable cavitation, **(B)** translation, and **(C)** inertial cavitation. The PI images show delivery from the extracellular space, while the post-US calcein images show cellular viability. **(D)** When characterized by change in bubble radius per unit time ($\Delta R/T_{US}$) versus total length of bubble displacement, the three groups are fairly well-distinguished. **(E & F)** The third type, inertial (transient) cavitation, driven by short pulse and high pressure, led to the highest delivery efficiency with the highest delivery rate and reasonably high viability.

US: Ultrasound.

Reproduced with permission from [54].

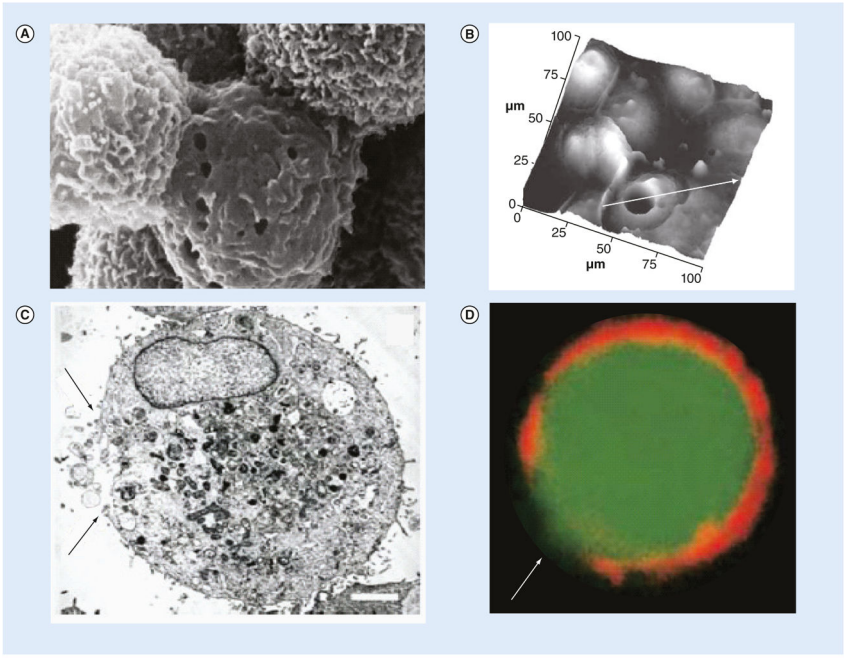

Figure 4. Direct observation of pore formation after sonoporation

Observations used **(A)** scanning electron microscopy, **(B)** atomic force microscopy, **(C)** transmission electron microscopy and **(D)** confocal fluorescence microscopy. **(A)** The magnification is 10,000 ×. **(B)** The white arrow passes through the pore; the cross-sectional plot over the line is given in [8]. **(C & D)** The scale bar is 1 μm, and the arrows point to the areas of cellular membrane disruption.

(A) Reproduced with permission from [56]; **(B)** Reproduced with permission from [8]; **(C & D)** Reproduced with permission from [9].

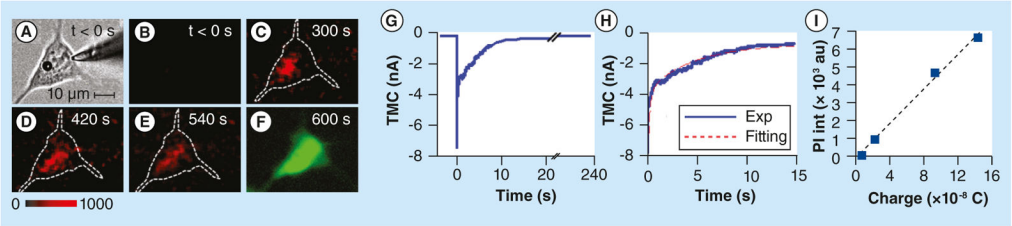

Figure 5. The entire dynamic process of pore opening and closing was monitored by transmembrane current in real-time using patch clamp technique and confirmed by the cell-impermeable fluorescent dye influx, diffusion inside the cell and stabilization

(A) Cell with round microbubble on left and patch clamp tip on right. **(B–E)** After ultrasound exposure, fluorescence imaging shows influx of propidium iodide (red) from extracellular space, while **(F)** green viability assay shows cell is alive. **(G–H)** Transmembrane current changes at the time of ultrasound exposure corroborating delivery. **(I)** Propidium iodide is proportional to the change in total charge suggesting diffusion-driven transport.

Reproduced with permission from [67].

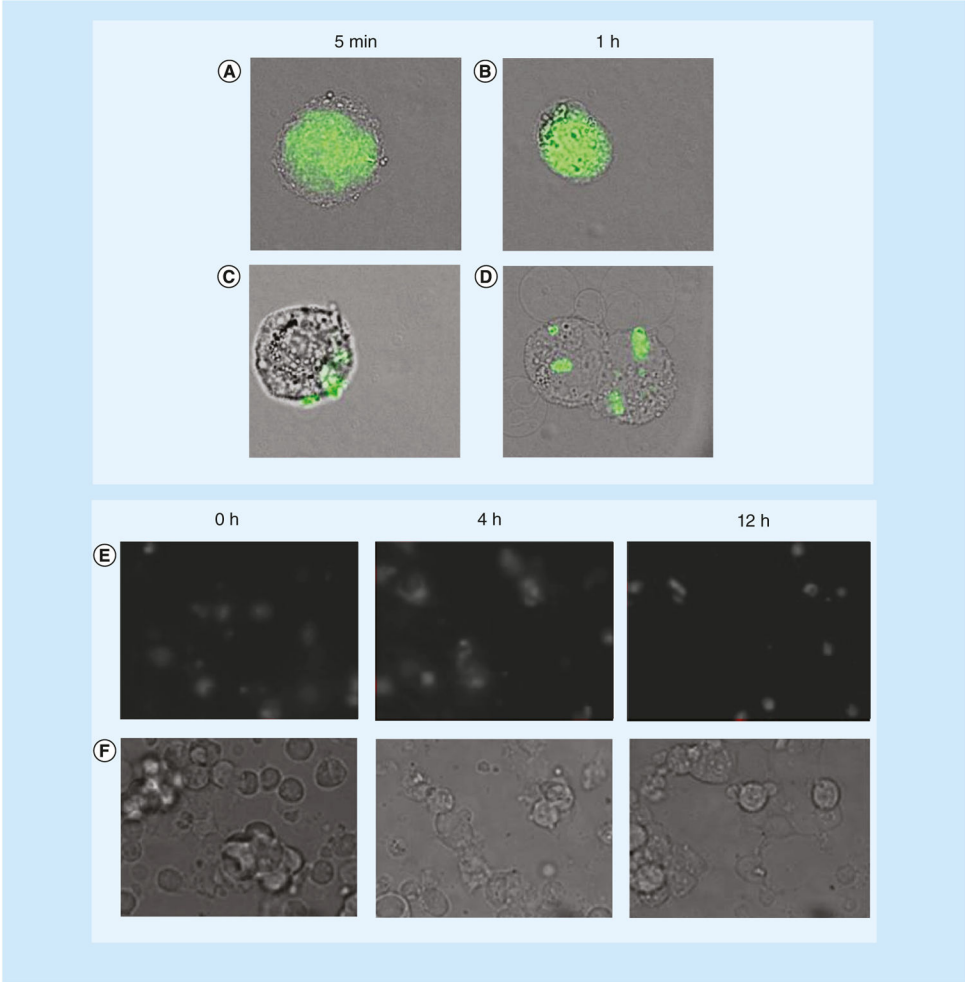

Figure 6. Intracellular kinetics of plasmids after sonoporation

(A & B) Fluoresently labeled plasmid DNAs show homogeneous distribution in rat mammary carcinoma cells (MAT B III) after sonoporation suggesting diffusion through pores while **(C & D)** the plasmids are concentrated in vesicles after lipofection, suggesting endocytosis. **(E & F)** At different time points after sonoporation, plasmid DNAs with fluorescent labels are homogenously distributed inside human embryonic kidney (HEK-293) cells after ultrasound exposure in the presence of microbubbles. **(A–D)** Reproduced with permission from [78]; **(B & F)** Reproduced with permission from [79].

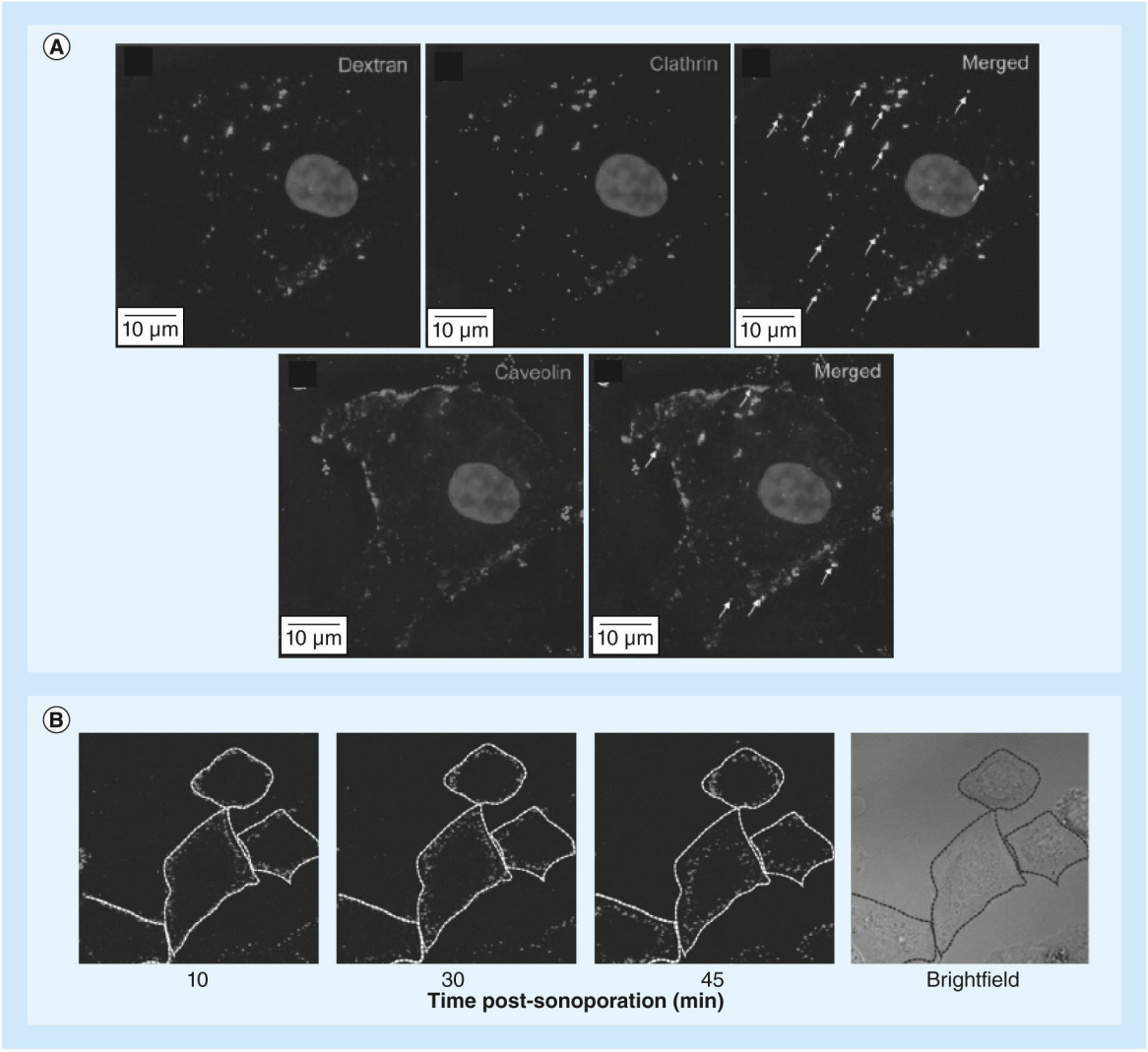

Figure 7. Large macromolecules may enter cells by endocytosis after ultrasound treatment

(A) Co-localization of 500 kDa dextran and endocytosis markers (clathrin and caveolin) after sonoporation. **(B)** Fluorescent-labeled plasmid DNA distribution and trafficking at 10, 30 and 45 min after sonoporation show that the vesicles move closer to the nucleus over time.

(A) Reproduced with permission from [76]; **(B)** Reproduced with permission from [38].